JOURNAL OF CATALYSIS **176,** 294–304 (1998)
ARTICLE NO. CA982027

Effect of Light on Reactions over Sulfated Zirconia

Alexander F. Bedilo,[1] Vladimir I. Kim, and Alexander M. Volodin

Boreskov Institute of Catalysis, Novosibirsk 630090, Russia

Received July 18, 1997; revised January 28, 1998; accepted January 29, 1998

The effect of illumination with visual and near-UV light on the isomerization and cracking of n-pentane and formation of radical cations from benzene and its derivatives over sulfated zirconia has been studied. Sulfated zirconia proved to have very strong acceptor sites capable of ionizing benzene and methylbenzenes to corresponding radical cations. The ionization of aromatic molecules could be initiated with visual light. The presence of oxygen in the gas phase appeared to strengthen the acceptor sites and shift the photoreaction red edge to longer wavelengths. Electron donor–acceptor complexes are shown to be key intermediates in the ionization of aromatic molecules on sulfated zirconia. A qualitative correlation between the presence of the strongest acceptor sites and the isomerization activity was observed. Illumination with visual light significantly increased the pentane cracking selectivity with little effect on the isomerization activity. Pentane cracking is proposed to proceed via dimerization initiated by the charge transfer with the formation of unstable radical cations. © 1998 Academic Press

INTRODUCTION

Skeletal isomerization of light normal paraffins is an important industrial reaction. It is known to require very strong acidity and is usually catalyzed by liquid superacids or Pt on chlorinated alumina. It is often used to test the strength of superacid catalysts (1). Despite a lot of effort, the isomerization mechanism remains disputable. The reaction is usually supposed to follow an ionic mechanism involving carbonium or carbenium ions formed by H^+ addition or H^- abstraction, respectively. However, radical cations are also often discussed as possible intermediates (2–6).

Sulfated zirconia has attracted considerable attention of researchers as a potential isomerization catalyst (5–16). It is more environmentally friendly and is more active at low temperatures than the systems currently in use (8). Brönsted (8, 16) and Lewis (9, 17) acid sites, their combination (10), as well as one-electron acceptor (oxidizing) sites (5, 6, 11) have been claimed responsible for its unique activity.

Until recently, high-silica zeolites were the only materials capable of ionizing adsorbed benzene (ionization potential 9.25 eV) to its radical cations (18–20). Sulfated zirconia has been also shown to initiate radical cation reactions of benzene (11, 21). However, primary benzene radical cations stabilized on surface active sites have never been observed by ESR. It can be explained by their high reactivity and lack of diffusion difficulties in sulfated zirconia pores, compared to zeolite channels.

Earlier, we have studied thermal and light-induced formation of benzene radical cations on ZSM-5 zeolites (19, 20, 22, 23). The reactions were shown to involve either thermal or photo-excitation of intermediate donor–acceptor complexes between molecular benzene and surface acceptor sites.

Photochemical generation proved to be an efficient way for the formation and investigation of primary radical cations. They can be stabilized at sufficiently low temperatures when subsequent reactions are hindered. In such a case one can eliminate thermal reactions, whereas the energetics of the photoreactions can be very informative for understanding the nature of primary adsorption complexes responsible for the light absorption.

An effect of visual light on the alkane isomerization over sulfated zirconia, if observed, would become strong evidence of the participation of strong surface acceptor sites in this reaction. To our knowledge, no photoreactions on sulfated zirconia catalysts have been reported to date.

In the present paper we report the results of our investigation of the effect of visual light on reactions over sulfated zirconia. Two processes have been studied: cracking and isomerization of n-pentane at room temperature and formation of radical cations from benzene and its derivatives.

METHODS

Two different samples of sulfated zirconia were used in this study. The first sample was prepared by a traditional method according to (10). Zirconium hydroxide was precipitated from aqueous solution of $Zr(NO_3)_2$ with aqueous ammonia, filtered, thoroughly washed with distilled water, and dried at 100°C overnight. The solid was treated with 0.2 N H_2SO_4 solution (5 cm^3/g) for 1 h at room temperature. Then the solid was filtered, dried without washing

---

[1] Corresponding author. E-mail: A.F.Bedilo@catalysis.nsk.su.

0021-9517/98 $25.00

overnight at 100°C, and calcined at 550°C for 3 h in air. The sample will be denoted below as SZ-1.

The second sample (hereafter denoted as SZ-2) was prepared as follows (24). Hydrous zirconia was precipitated from a $ZrOCl_2$ solution with aqueous ammonia, thoroughly washed with distilled water, dried overnight at 100°C, and calcined at 500°C for 3 h. The resulting zirconium oxide (60 m^2/g) was impregnated with aqueous $(NH_4)_2SO_4$ to give nominal sulfur loading equivalent to 2.5 sulfur atoms per nm^2, dried without washing, and calcined at 500°C for 3 h.

Benzene, toluene, and p-xylene of "pure" degree were purified by a freeze-pump-thaw procedure. Pentane ("pure" degree) was purified from olefins and aromatic compounds according to (25). Then it was stored over a zeolite.

ESR experiments were conducted in our ESR *in situ* installation described elsewhere (23). One-tenth gram of a catalyst was placed in a quartz ampoule connected to a high-vacuum system. The standard sample pretreatment included alternating oxygen–vacuum treatments at 500°C in a vacuum line with a trap cooled by liquid nitrogen. The final pretreatment step was a 2-h heating in oxygen (10 Torr) with subsequent cooling to room temperature and evacuation for 20 min. Desired amounts of hydrocarbons were adsorbed from the gas phase.

A monochromator used made it possible to study spectral characteristics of the photoreactions in the energy range of 1–5 eV. The ESR samples were subjected to the illumination directly in the spectrometer cavity. A 1-kW mercury lamp served as the irradiation source.

Isomerization was conducted in sealed glass reactors containing 200 mg of the catalyst and 5 ml of pentane at 30°C under argon or oxygen atmosphere. The reaction mixture was vigorously stirred with a magnetic stirrer. Before the reaction, the catalyst was evacuated at 300°C for 2 h.

When desired, the reaction mixture was quickly cooled to 77 K. Then it was analyzed by gas–liquid chromatography (3 m 5% Apieson L on Chromosorb PAW—DMCS) and GC-MS.

Textural characterization of the samples was performed on a NOVA 1200 gas sorption analyzer (Quantachrome Corp.). Prior to the analysis, the samples were outgassed at 180°C for 1 h. Seven point BET surface areas, total pore volumes, and pore size distributions (BJH method) were calculated from 40 point nitrogen adsorption–desorption isotherms.

X-ray powder diffraction experiments were conducted on a Scintag-XDS-2000 spectrometer with Cu Kα radiation. Scans were made in the 2Θ range 20–80° with a scanning rate 1° per minute. Crystallite sizes were determined from the X-ray line broadening using Scherrer's equation. Volume fractions of zirconia tetragonal and monoclinic phases were calculated from integrated peak intensities.

Thermogravimetric analysis (TGA) was performed on a Shimadzu TGA-50 instrument. The samples were heated in platinum crucibles up to 1000°C with a heating rate 10°C per minute in 30 ml/min dry air flow.

RESULTS

Characterization of Samples

It is generally believed that active sulfated zirconia catalysts can be prepared only by the impregnation of amorphous zirconia. The use of a crystallized support usually does not lead to samples with appreciable activity. A couple of major important exceptions (12, 13) only support the rule. The first sample studied in the present article (SZ-1) was prepared following the original preparation technique (7). It was interesting to compare its properties with those of the other sample prepared by impregnation of crystalline ZrO_2 (SZ-2), which also possesses relatively high acidity and has a similar chemical composition.

Figure 1 presents XRD spectra of the samples studied. SZ-1 shows only a pattern typical to the tetragonal phase of ZrO_2 (12). This result is consistent with most studies of active sulfated zirconia. The introduction of sulfate species is known to stabilize the metastable tetragonal phase up to 700°C. The average crystallite size was determined from the reflex width to be 95 Å.

SZ-2 shows a superposition of monoclinic and tetragonal phases of ZrO_2. The most intensive peaks of these phases are marked as **m** and **t**, respectively (Fig. 1). Their ratio

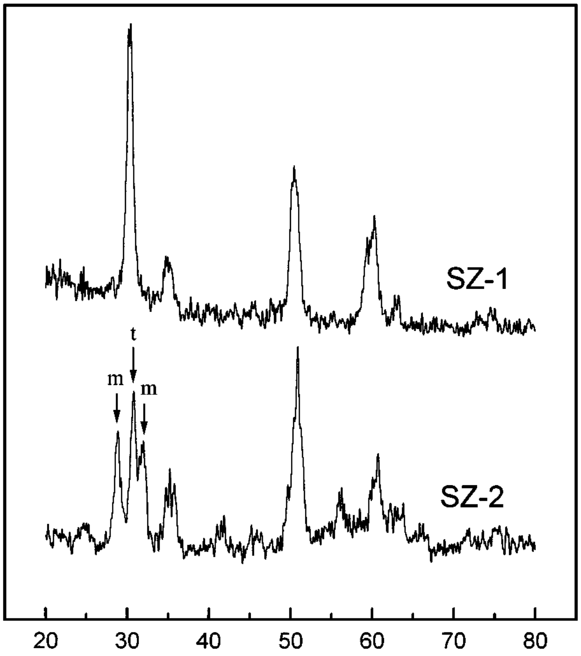

FIG. 1. XRD spectra of the catalysts.

may be evaluated from the relative integral peak intensities (26) as 4 : 1. The zirconia support had been precalcined at 500°C—high enough to convert most of the tetragnoal phase to the thermodynamically stable monoclinic phase (27, 28). Sulfation of such mixture hardly has any influence on the phase composition. Definitely it cannot reverse the process of transition from the tetragonal to the monoclinic phase and sometimes (12) is even believed to facilitate it. The average particle size determined for the monoclinic phase was larger than that of SZ-1—140 Å.

Characterization of the samples by BET has shown that the samples have the porous structure typical for respective types of sulfated zirconia. The surface area of SZ-1 is more than twice as high as that of SZ-2—135 and 60 m^2/g, respectively. These data correspond well with those reported. Total pore volumes of the samples are 0.15 and 0.10 cm^3/g, respectively.

TGA spectra of the samples in the region above 500°C are shown in Fig. 2. Below 500°C only a peak of physisorbed water is observed at $T < 100°C$. The high temperature peak has been shown to correspond to the decomposition of sulfate species (29). According to MS studies, only SO_2 and O_2 are usually evolved during the thermal decomposition under oxidizing conditions. As most of the water is lost at lower temperatures, it is reasonable to assume that the overall decomposition reaction in air at high temperatures corresponds to the evolution of SO_3, which is subjected to further decomposition (29). Furthermore, the molar amount of sulfur calculated with this assumption practically matches the amount introduced into SZ-2 during the sulfation procedure—2.1 wt% (of SO_3). The SO_3 loading in SZ-1 was determined from the weight loss as 4.6 wt%. Both correspond to the same surface concentration of 2.5 sulfur atoms per nm^2.

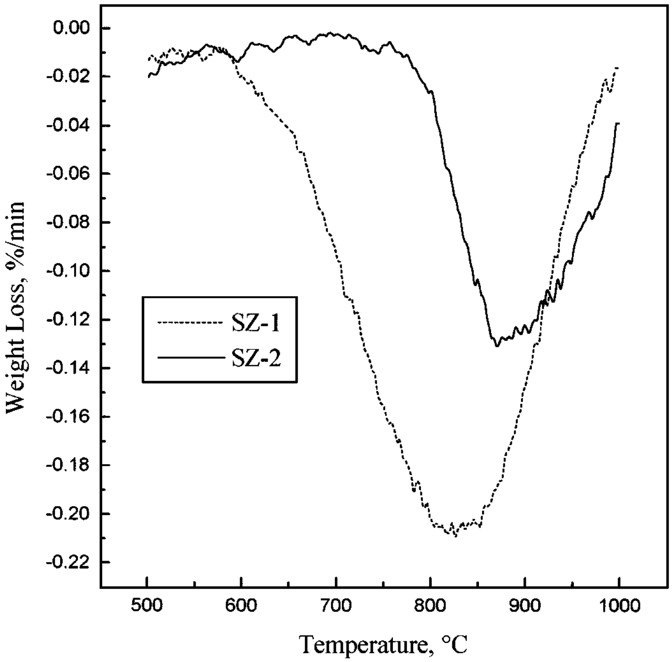

FIG. 2. Derivative TGA spectra in the temperature range of 500–1000°C.

If we assume that each sulfate group occupies 25 Å (10), the concentration of sulfates in our samples would be about 60% of a nominal monolayer. Previously, close to monolayer loadings were found necessary to obtain the maximum isomerization activity (10, 30) and the maximum concentration of paramagnetic species formed after adsorption of aromatic molecules (24).

The difference in the positions of the decomposition maxima of the samples is another interesting feature of the TGA spectra. In SZ-1 the decomposition peak is centered at 825°C, whereas in SZ-2 it has a maximum at 870°C. This effect cannot be ascribed only to the difference in the amount of sulfates. First, both correspond to almost the same surface concentration. Second, one would expect the apparent decomposition peak to shift to higher temperatures with an increase in the sulfate concentration if the heating is too fast. Obviously, in SZ-1 the bonding energy of sulfates with the zirconia surface is substantially lower than in SZ-2. Active sulfated zirconia catalysts are known to contain covalent sulfates (9). It is very likely that covalent sulfates of SZ-1 decompose around 825°C, whereas sulfates in SZ-2 decomposing at higher temperatures are more ionic. Our scanning of a wide selection of sulfated zirconia catalysts prepared by different methods have shown that the most active samples have a monolayer sulfur loading with the decomposition peak around 830°C (30).

Formation of Radical Cations from Adsorbed Aromatic Molecules

Trained outgassed samples of both catalysts exhibited only a weak axial spectrum with $g_\perp = 1.98$ and $g_\parallel = 1.95$ which can be assigned to Zr^{3+} ions, as in (11). The signal could be reversibly broadened by oxygen indicating that the ions are located on the surface and not in the bulk. The same regards all the other radicals discussed below. The signal was not observed to change in the hydrocarbon adsorption process.

The formation of radical species during adsorption of aromatic hydrocarbons on catalytic surfaces is often used as a test of the strongest acceptor sites (11, 31). Often only broad poorly resolved spectra are observed. Sometimes it is questioned if they result from transformations of primary radical cations (32). Therefore, it is important to identify primary particles and to study their graduate transformations to elucidate their input into the overall paramagnetism.

To detect primary particles formed in the course of benzene adsorption on sulfated zirconia, experiments at low temperature and adsorbate coverage were conducted. These conditions hinder secondary reactions and are

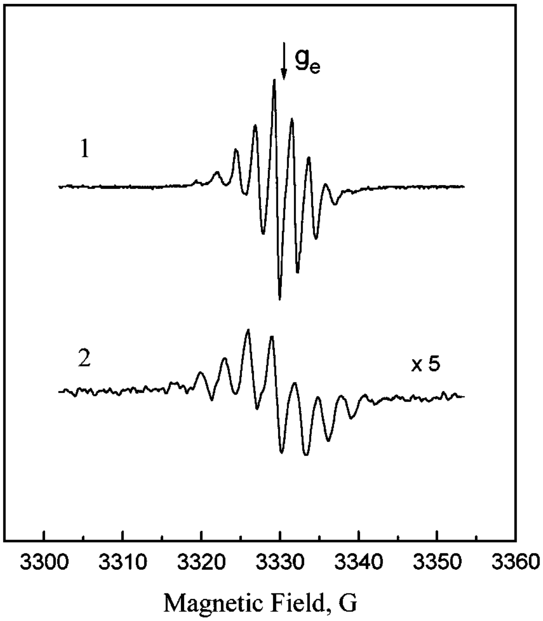

FIG. 3. ESR spectra registered after adsorption of benzene vapor on SZ-1 at 243 K (1) and in 30 min after heating up to room temperature (2).

favorable for registration of primary radical cation intermediates.

Benzene adsorption on SZ-1 in the amount of 0.5 mmol/g of the catalyst at 233 K resulted in the formation of benzene dimer radical cations (Fig. 3, Spectrum 1) with a characteristic hyperfine constant $a = 2.2$ G. They are formed due to a close interaction of benzene radical cations with neutral molecules and are known for benzene adsorbed on zeolites (33). Upon heating to room temperature they quantitatively transformed into biphenyl radical cations with $a = 3.3$ G (Fig. 3, Spectrum 2). Naturally, only these particles were observed when the adsorption was performed at room temperature (11, 24). The ESR parameters of the radical cations practically coincide with the parameters of analogous particles formed from benzene on a ZSM-5 zeolite (20).

Only secondary radicals were observed during toluene adsorption on SZ-1 even at 200 K. In this case, we did not manage to register primary radical cations. They are known to be even less stable than benzene radical cations. Only products of their oxidative dimerization—4,4-dimethylbiphenyl radical cations—were registered after toluene adsorption on a mordenite zeolite (33). In our system, even these particles were not observed. The radicals stabilized (Fig. 4, Spectrum 1) are likely to result from the deprotonation of the above radical cations. A simulated spectrum of these radicals is also shown in Fig. 4 (Spectrum 2). The spectrum was simulated with the following reasonable parameters $g = 2.00365$, $a^1_\perp = 8.2$ G, $a^1_\parallel = 8.85$ G, $a^2 < 0.2$ G, $a^3_\perp = 2.5$ G, $a^3_\parallel = 2.8$ G, $a^4_\perp = 2.7$ G, $a^4_\parallel = 2.8$ G. A proposed scheme of this process is shown below.

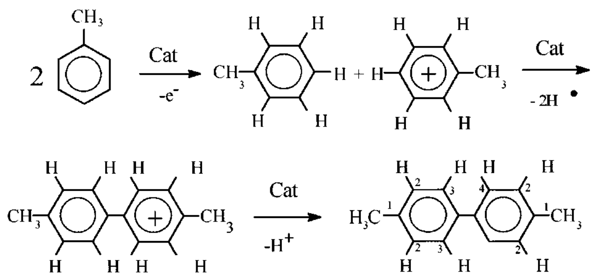

At room temperature it took several hours for the radicals to transform into particles with poorly resolved hyperfine structure (Fig. 4, Spectrum 3). These particles are likely to result from polycondensation of the radicals with toluene molecules. The reactions proceeded much faster if toluene was present in the gas phase.

The concentration of the radicals was observed to depend on the amount of toluene adsorbed (Fig. 5). As on ZSM-5 zeolites (19), the process was completely reversible. The radical concentration reversibly decreased if the sample was pumped out. The plateau on the curve seems to reflect the total concentration of surface sites capable of ionizing toluene.

Earlier electron donor acceptor complexes have been proposed to be key intermediates in the formation of

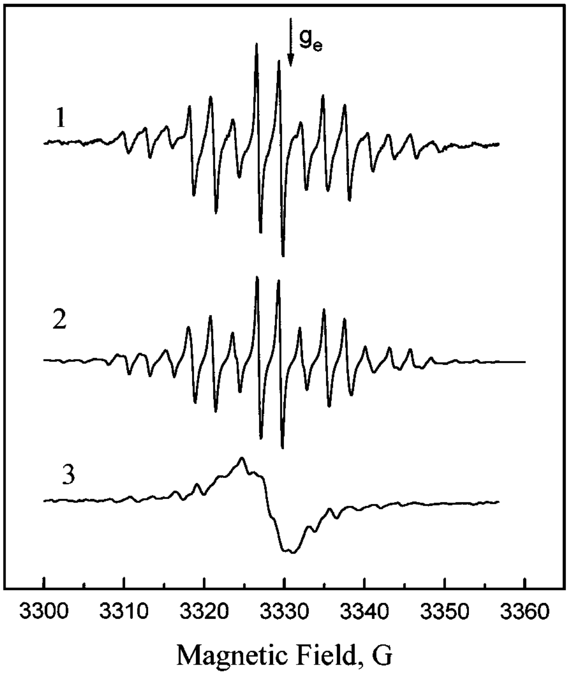

FIG. 4. ESR spectra registered after adsorption of toluene vapor on SZ-1 at 243 K (1), in 30 min after heating up to room temperature (3) and a spectrum simulated with parameters listed in the text (2).

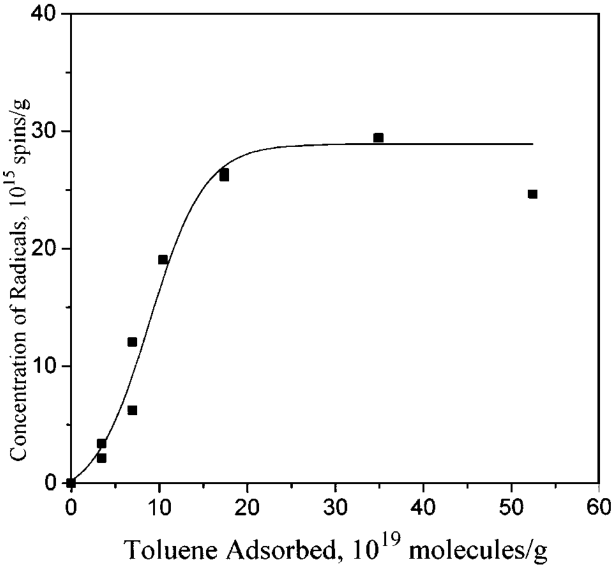

FIG. 5. Dependence of the concentration of radicals on the amount of toluene adsorbed on SZ-1 at 243 K.

aromatic radical cations ($\mathbf{Ar}^+$) on surface acceptor sites ($\mathbf{A}_s$) (20, 24):

$$\begin{tikzcd} \mathbf{Ar} + \mathbf{A_s} \arrow[r, shift left] & {[\mathbf{Ar} \bullet \mathbf{A_s}]} \arrow[l, shift left] \arrow[r, shift left] & {[\mathbf{Ar}^+ \bullet \mathbf{A_s^-}]^*} \arrow[l, shift left] \arrow[r] & \mathbf{Ar}^+ + \mathbf{A_s^-} \arrow[ll, bend left] \end{tikzcd}$$

Reversible disappearance of the radical cations must result from the shift in the equilibrium caused by desorption of adsorbed molecules under continuous evacuation.

Earlier, acceptor sites of H-ZSM-5 zeolites were shown to incorporate chemisorbed oxygen (19). Here oxygen also appeared to strengthen the acceptor sites. Introduction of oxygen to any sample described above led to a fast formation of intensive spectra of polycondensed aromatics. Without oxygen, they are formed only at higher temperatures in excess of aromatic molecules (21).

The effect of oxygen is even more pronounced for SZ-2. This sample appeared to have weaker acceptor sites. No radicals were formed after adsorption of benzene or toluene on SZ-2 in the absence of oxygen. Its presence in the gas phase is required to initiate their ionization with the formation of the same radicals as described above. The concentration of the radicals appeared to depend on the amount of oxygen introduced (Fig. 6).

SZ-2 proved to be a convenient sample for the investigation of radical cations formed on its surface. First, its acceptor sites are much stronger than those of conventional solid acids and comparable with those of high-silica zeolites. Second, these sites are accessible to large molecules. Third, the radical species formed are much more stable than on a stronger SZ-1.

We observed the formation of secondary radical particles derived from primary radical cations after adsorption of different benzene derivatives on its surface. Sometimes, primary radical cations were reasonably stable, and well-resolved spectra could be observed.

In the case of p-xylene no oxygen was required for the formation of radical cations. The adsorption of pure p-xylene gave spectra with hardly resolvable hyperfine structure. But we managed to observe a well-resolved spectrum by adsorbing its diluted solutions in benzene and toluene. As radical cations of substances with lower ionization potentials are known to substitute those of compounds with higher ionization potentials, only p-xylene radical cations were observed.

A typical ESR spectrum of p-xylene radical cations is presented in Fig. 7, Spectrum 1. One can see a well-resolved hyperfine structure attributable to two groups of equivalent protons ($a_1 = 15.8$ G; $a_2 = 2.0$ G). Like the other particles presented above, they quickly transformed at room temperature into a broad ($\Delta H = 6$–10 G) line without any detectable hyperfine structure, its form being typical for heavier oligomers known to be coke precursors. The radical-cationic oligomerization proved to be very favorable for benzene from the energetic point of view (34) and seems to proceed quickly in these cases as well. In contrast to zeolites, no steric difficulties exist here.

Hexamethylbenzene (HMB) radical cations proved to be stable for several days even at room temperature as the oligomerization is unlikely for them (Fig. 7, Spectrum 2). The parameters of their spectrum are $g = 2.0028$, $a = 6.30 \pm 0.05$ G, $\Delta H = 0.50 \pm 0.05$ G. Only 15 of 19 lines were observed, their relative intensities correlating well with the expected ones. Small deviations result from the A-tensor anisotropy. The figures are close to those reported by Hulme and Symons (35), who were the first to observe HMB radical cations in sulfuric acid under irradiation. The fact that only HMB radical cations were observed in all the

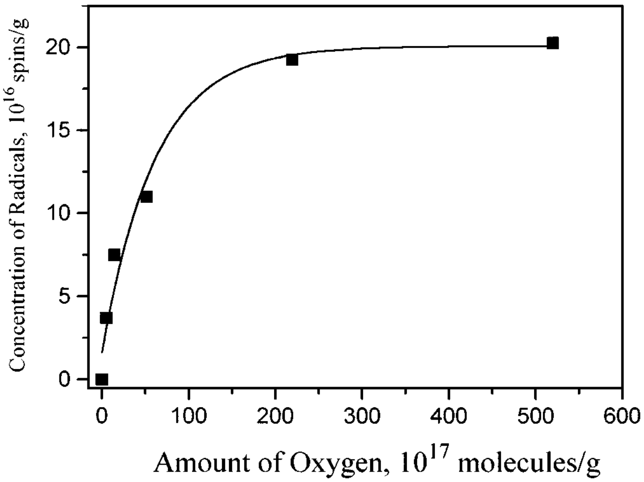

FIG. 6. Dependence of the concentration of radicals after toluene adsorption on SZ-2 at 243 K on the amount of oxygen introduced.

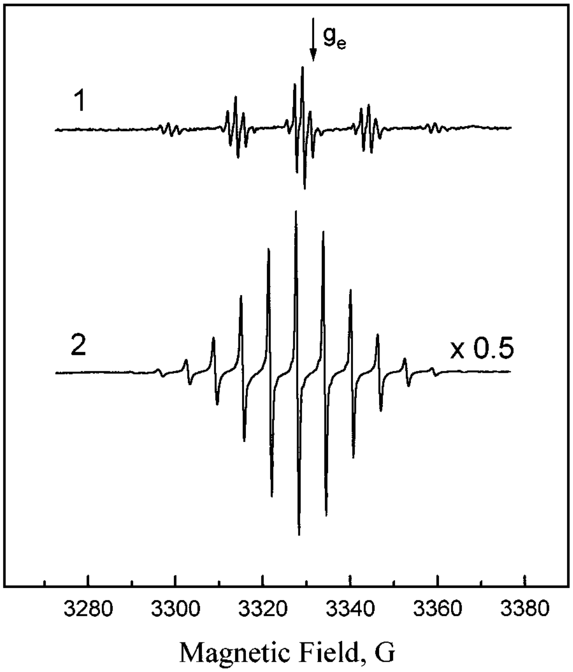

FIG. 7. ESR spectra registered on SZ-2 at 293 K after adsorption of a 100 : 1 gaseous benzene-para–xylene mixture without oxygen (1) and a 10^{-2} *M* hexamethylbenzene solution in benzene in air (2).

solvents even at its concentration as low as 10^{-4} M, when the number of HMB adsorbed is close to the number of radical cations generated, confirms the radical cation origin of the particles resulting from the benzene and toluene adsorption.

Side by side with primary radical cations and products of their chemical transformations, O_2^- radical anions ($g_{xx} = 2.003$; $g_{yy} = 2.010$; $g_{zz} = 2.031$) were observed if oxygen was present in the system. The g_{zz} value of the radical anions suggests that they are localized on tetravalent ions, certainly Zr^{4+} (11, 36). Without a hydrocarbon no radical anions were detected. These particles might result from the electron transfer from the hydrocarbon. However, no straightforward dependence between the concentrations of the oxygen radical anions and aromatic radical cations was observed.

Light-Induced Formation of Radical Cations

It is well known that electron donor–acceptor complexes can be excited not only thermally but also by illumination. Earlier we showed that benzene radical cations could be generated with blue light on a ZSM-5 zeolite (23). Illumination with visual light proved to be an efficient way of generating radical cations on sulfated zirconia as well.

As stated above, benzene adsorption on SZ-2 did not result in the formation of any paramagnetic species. In an attempt to register primary benzene radical cations, we pumped out excess benzene at 0°C. A thermal desorption experiment showed that sufficient amount of benzene remained adsorbed on the surface. The visual light illumination was conducted at 103 K. Radical cations formed under illumination proved to be stable at this temperature under vacuum for at least several hours.

A weak spectrum of benzene radical cations could be observed after a 5-min illumination with green light (546 nm) (Fig. 8, Spectrum 1). This concentration could be increased by an order of magnitude by a prolonged irradiation with $\lambda = 365$ nm (Fig. 8, Spectrum 2). The radical cations observed have a visible anisotropy of **g** and **a** tensors. The spectra can be simulated as 6 equivalent protons with $g_\perp = 2.0029$, $g_\parallel = 2.0024$, $a_\perp = 4.2$, $a_\parallel = 5.0$ (Fig. 8, Spectrum 3). These parameters differ from those observed on H-ZSM-5 (22, 23), where no anisotropy is detected, but they are close to those of benzene radical cations formed on HY zeolites under γ irradiation (37). The anisotropy could result from the stabilization of the radical cations on Zr^{4+} ions.

Introduction of oxygen did not lead to the formation of paramagnetic particles at a low benzene coverage. However, it did change the spectral characteristics of the photoprocess. Figure 9 presents the concentration of radicals formed after illumination of the same sample for 1 min with the selected light at different oxygen pressures. The concentration appeared to increase with an increase of the oxygen pressure up to several torr. It is notable that a detectable concentration of radicals was generated with yellow light (579 nm) only when some oxygen was

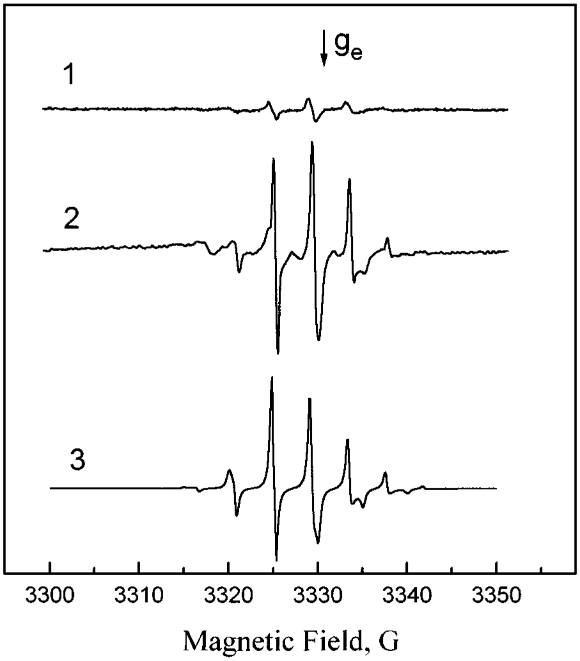

FIG. 8. ESR spectra registered after benzene adsorption on SZ-2 at room temperature, evacuation for 30 min at 273 K and illumination at 103 K with $\lambda = 546$ nm for 5 min (1) and with $\lambda = 365$ nm for 30 min (2); and a simulated spectrum of benzene radical cations (3).

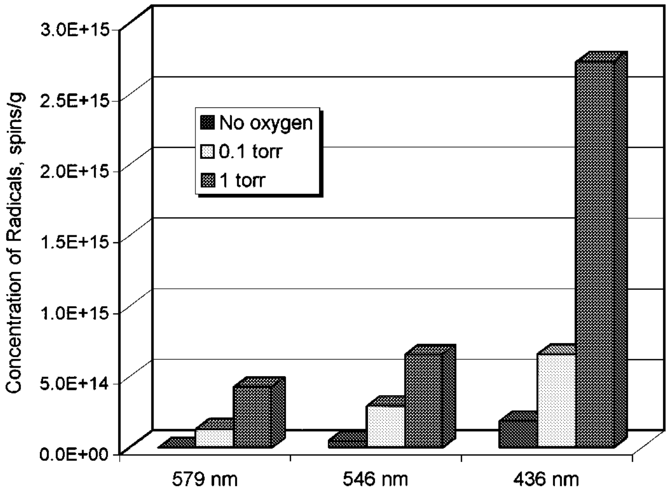

FIG. 9. Concentration of benzene radical cations formed after benzene adsorption on SZ-2 at room temperature, evacuation for 30 min at 273 K and illumination with selected light for 1 min at 103 K in the absence of oxygen and with 0.1 and 1 Torr of oxygen.

present. Oxygen seems to strengthen the surface acceptor sites, resulting in the thermal ionization of benzene and toluene on SZ-2 and red shift of the light-induced ionization.

The amount of adsorbed benzene was also found to affect the spectral characteristics of the light-induced formation of radical cations. If the sample was not evacuated as in the above experiments, benzene dimer radical cations were generated under illumination (Fig. 10). It is important that their concentration was higher than that of benzene radical cations formed during illumination of the evacuated sample under the same conditions, and the red edge of the photoprocess was obviously shifted to longer wavelengths (Fig. 11). This effect is analogous to the influence of the amount of adsorbed hydrocarbons on the concentration of the radical cations generated thermally and is one more evidence of the similarity between thermal and light-induced processes in this system.

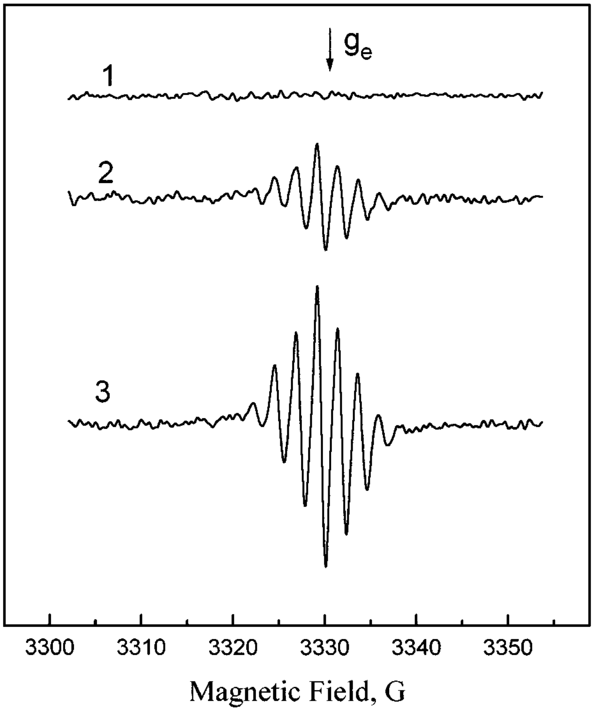

FIG. 10. ESR spectra observed at 103 K after benzene adsorption on SZ-2 (1) and illumination for 1 min with $\lambda = 546$ (2) and 436 (3) nm.

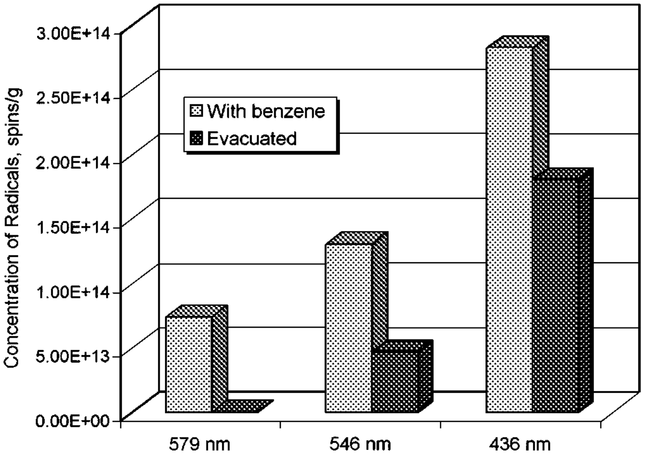

FIG. 11. Concentration of benzene radical cations formed during illumination with selected light for 1 min at 103 K on SZ-2 with adsorbed benzene and after evacuation for 30 min at 273 K.

Photoionization could be effectively used for the generation of radical cations on SZ-1 as well. In this case we could not realize the situation when no radicals are observed after adsorption of benzene derivatives. However, difference spectra unambiguously show the formation of radical cations under illumination. Figure 12 presents in a real scale spectra of benzene dimer radical cations formed after adsorption (1) and difference spectra after a 2 min illumination with $\lambda = 436$ nm (2) and 365 nm (3).

Two facts are notable. First, the visual light illumination gives rise to the same benzene dimer radical cations as those formed thermally. Second, the concentration of the radical cations generated in this case is significantly higher than in the case of SZ-2.

An analogous effect was observed with other aromatic molecules studied. Figure 13 exemplifies it for a p-xylene–benzene mixture in the absence of oxygen. The concentration of p-xylene radical cations both thermal and light-induced was higher than in the case of benzene. This effect is reasonable in view of a lower ionization potential of p-xylene.

Thus, both sulfated zirconia samples are shown to possess very strong one-electron acceptor sites. However, the fact that oxygen is required for ionization of benzene and toluene on SZ-2 marks a significant difference in their acceptor strength. In general, the strength of the strongest

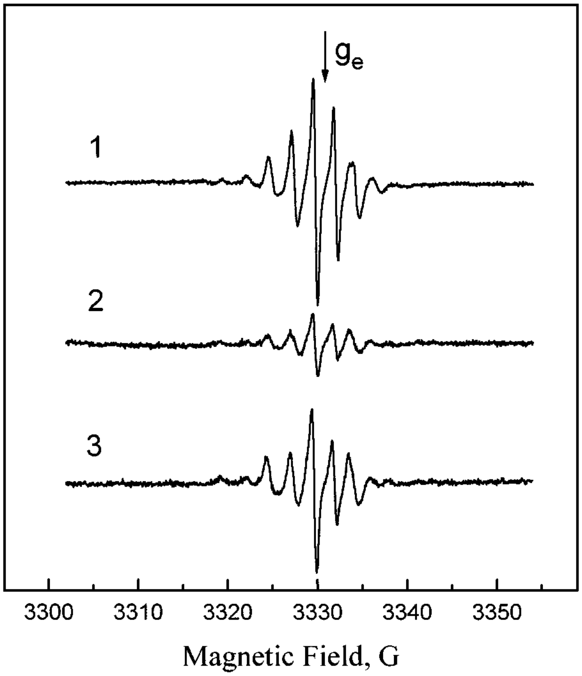

FIG. 12. ESR spectra observed at 233 K after benzene adsorption on SZ-1 and evacuation at 273 K (1) and difference ESR spectra corresponding to radical species added by illumination for 2 min with $\lambda =$ 436 nm (2) and $\lambda = 365$ nm (3).

acceptor sites of SZ-2 seems to be close to that of high-silica zeolites, whereas SZ-1 appears to possess the strongest one-electron acceptor sites among all oxide materials known. Aromatic molecules and the acceptor sites are shown to form surface donor–acceptor complexes, which can be excited both thermally and by illumination to yield radical cations.

Effect of Light on the Isomerization and Cracking Activity

To check if the strong surface acceptor sites discussed above play an important role in the isomerization catalytic activity of sulfated zirconia, we decided to examine an influence of the visual light illumination on the catalytic activity. As shown above, benzene radical cations could be generated on the surface by the illumination with visual light. Although pentane is not an aromatic compound and has a higher ionization potential, there was a certain chance that its donor–acceptor complexes with the surface acceptor sites would absorb in the visual spectral region. Therefore, if the visual light illumination had a significant effect on the catalytic activity, this would become a strong support of the idea (5, 6) that alkane radical cations formed on strong surface acceptor sites of sulfated zirconia are key intermediates in the isomerization reaction pathway.

SZ-1 catalyzed isomerization of n-pentane to isopentane at 30°C in Ar with a 98–99% selectivity at a 23% conversion in 2 h (Fig. 14A). The isomerization reaction kinetics in conversion versus time coordinates can be easily approximated by a straight line passing through the origin. Hence, the reaction rate did not change much during the whole 2-h run with the total conversion to isopentane about 10 mmol. Then, the reaction rate can be estimated to be 25 mmol g^{-1} h^{-1}. Isobutane and isomeric hexanes with the molar ratio $[i\text{-}C_4]/\sum[i\text{-}C_6] \approx 1$ were formed as by-products.

When the reactor was filled with oxygen instead of argon, no apparent changes in the activity or selectivity were observed. Illumination in argon also had little effect on the reaction rate. However, interesting results were obtained during illumination of n-pentane with sulfated zirconia in the oxygen atmosphere. The isomerization activity did not significantly depend on the illumination. Its slight increase was observed only in the near-UV region (365 nm) (Fig. 14A). However, the amount of isobutane and isomeric hexanes increased considerably already under yellow light (579 nm) (Fig. 14B). An obvious induction period was observed. Then the reaction rate appeared to increase with time. For example, the average isobutane formation rate under green light illumination (546 nm) between 1.5 and 2 h was about 1.0 mmol g^{-1} h^{-1}. The isobutane selectivity after 2 h under the 365 nm irradiation was six times higher than in the dark. Meanwhile, the isobutane/i-hexanes ratio remained unchanged.

SZ-2 showed a significantly lower activity, with pentane conversion about 1% after 2 h under the same conditions.

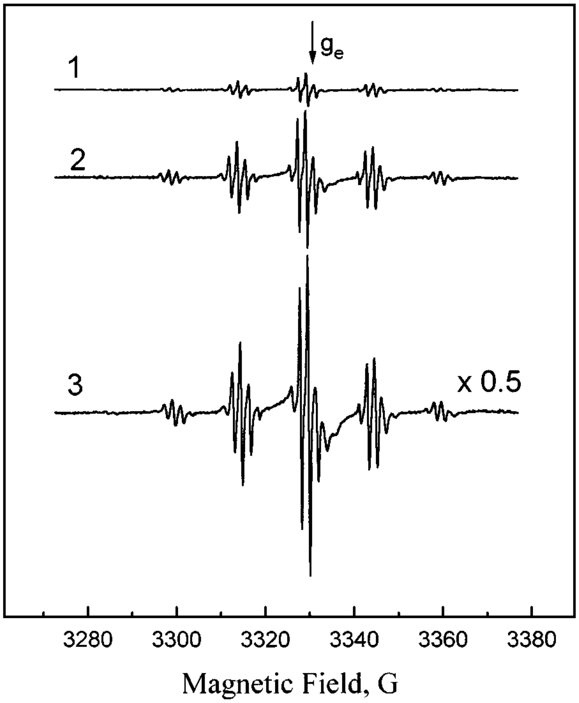

FIG. 13. ESR spectrum observed at 293 K after adsorption of a 100 : 1 gaseous benzene-p-xylene mixture (1) and difference ESR spectra corresponding to radical species added by illumination for 2 min with $\lambda = 436$ nm (2) and $\lambda = 365$ nm (3).

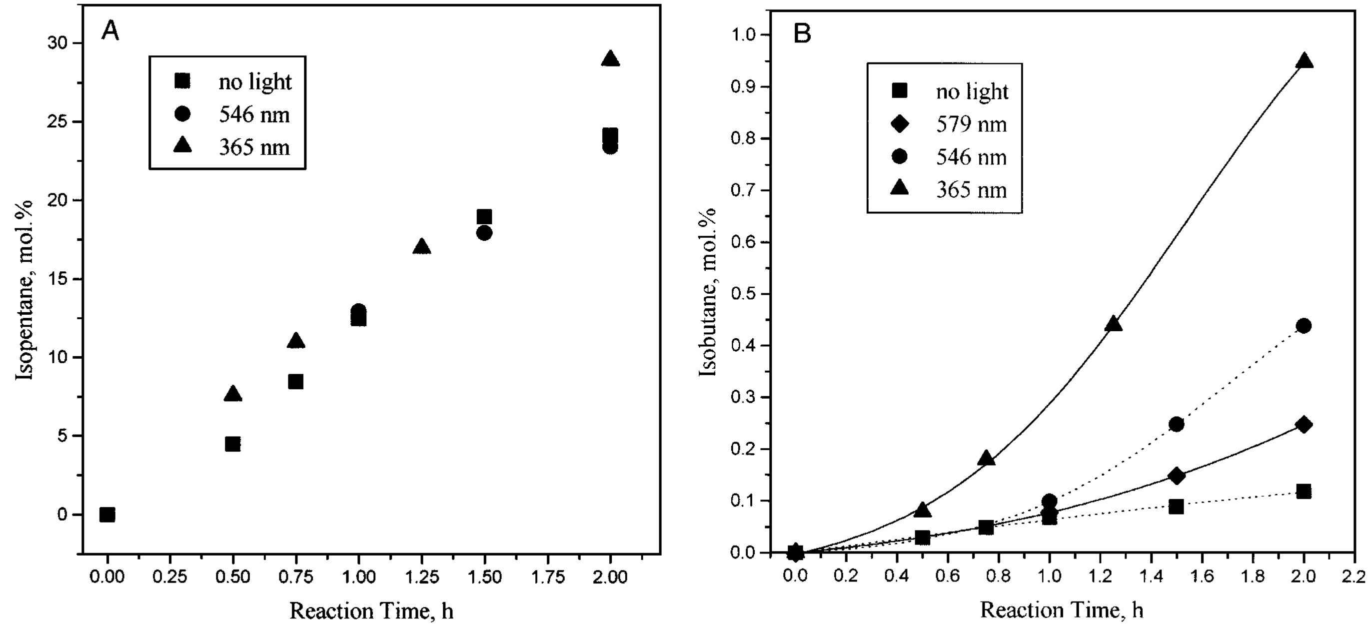

FIG. 14. Effect of light on the isomerization (A) and cracking (B) activity of SZ-1.

Therefore, the effect of illumination was not studied for this sample.

DISCUSSION

Sulfated zirconia is shown to possess very strong acceptor sites capable of ionizing benzene and its derivatives to their radical cations. As on zeolites, the process involves the excitation of intermediate surface donor–acceptor complexes, which can occur thermally or under illumination with visual light. Their formation results in a decrease of energy required for the ionization of small aromatic molecules, allowing their thermal ionization and significantly shifting the photoionization red edge to the visual spectral region.

The concentration of radical cations formed thermally appears to depend on such factors as strength of surface acceptor sites, ionization potential (donor ability) of aromatic molecules, the amount of hydrocarbon adsorbed and the presence of molecular oxygen in the system. The latter seems to participate in the donor–acceptor complexes and strengthen the acceptor sites.

It is notable that only a small portion of adsorbed molecules (less than 0.02%) is ionized. An analogous situation was observed on H-ZSM-5 zeolites (19). It seems that an "island" of liquid phase of a certain size is required for the generation of radical cations. The presence of the "liquid island" may decrease the energetic ionization barrier due to solvating effects and facilitate the charge separation by providing better transport conditions.

The red edge of the light-induced processes is well beyond the limits of any adsorption band of the catalyst or adsorbates. In fact, lower light energies were required in this system than in the case of similar processes on zeolites (22, 23), proving that sulfated zirconia has stronger acceptor sites. The red edge and the concentration of radical cations generated under illumination with a certain wavelength appear to depend on the same factors as the thermal formation of radical cations. All these factors taken separately and all together prove that electron donor–acceptor complexes are key intermediates in the thermal and light-induced formation of radical cations on sulfated zirconia:

$$\mathbf{D} + \mathbf{A_s} \rightleftarrows |\mathbf{D} \bullet \mathbf{A_s}| \qquad [1]$$

$$[\mathbf{D} \bullet \mathbf{A_s}] \overset{kT,h\nu}{\rightleftarrows} [\mathbf{D}^{+} \bullet \mathbf{A_s^{-}}]^{*} \qquad [2]$$

$$[\mathbf{D}^{+} \bullet \mathbf{A_s^{-}}]^{*} \overset{\nwarrow}{\longrightarrow} \mathbf{D}^{+} + \mathbf{A_s^{-}}. \qquad [3]$$

The above scheme generally describes the process of generation of radical cations via the excitation of surface donor–acceptor complexes. The first stage represents the formation of an electron donor–acceptor complex between an organic donor molecule (**D**) and a surface acceptor site ($\mathbf{A_s}$). On the second stage the complex undergoes thermal or photo excitation, with the charge separation and stabilization of a radical cation ($\mathbf{D}^{+}$) on the third stage. The scheme assumes that all the stages are reversible, and the whole process can be completely reversed, for example, by an evacuation of the sample.

Oxygen is not required for the generation of the photoactivity, but it does shift the absorption band to lower energies. This fact marks a significant difference between our system sensitive to the visual-light illumination and those studied by Frei *et al.* (38, 39). Their investigations of electron donor–acceptor complexes between oxygen and hydrocarbons in zeolites present the only other examples where charge-transfer bands in complexes with participation of small hydrocarbons could be so significantly shifted to lower energies by the presence of a catalyst. However, in their system oxygen is the only acceptor, and the band energies are shifted due to the stabilizing effect of zeolite supercages. In our case, oxygen only strengthens acceptor sites already present on the surface of sulfated zirconia. Also, as sulfated zirconia does not have a zeolite channel system, it is very unlikely that it could have a similar stabilizing effect on donor–acceptor complexes. The nature of its effect must be different.

As on zeolites and in the majority of homogeneous systems (40), the counter ion ($\mathbf{A}_\mathbf{s}^-$) is not observed by ESR. Therefore, its exact nature remains unclear. In the case of zeolites, there is a common opinion that oxidation occurs on Lewis sites (20, 40). Brönsted acidity itself is usually believed to be not sufficient for the generation of radical cations, the presence of an oxidizer being required. However, aromatic molecules with low ionization potentials, e.g. anthracene or perylene, are readily oxidized in concentrated sulfuric acid or in strong Brönsted acids in the presence of such weak electron acceptor as atmospheric oxygen (40).

The formation of donor–acceptor complexes presumes that a Lewis acid site is a part of the acceptor site. But numerous IR studies have shown that Lewis acid sites of sulfated zirconia are only slightly stronger than those of pure zirconia (41, 42). It is a simultaneous presence of strong Brönsted acid sites that makes sulfated zirconia different. Therefore, we believe that an acceptor site contains a strong Lewis site, a strong Brönsted site, and an electron trap located close to each other. The exact localization of electrons abstracted from the donor is unknown. Near-surface defects, surface low-coordinated zirconium ions, hydroxyl groups, and partly reduced sulfate groups can serve as such electron traps, which are not observed by ESR. When oxygen is present in the gas phase, ESR spectra of O_2^- radical anions stabilized on Zr^{4+} ions are observed, together with the aromatic radical cations. Adsorbed oxygen seems to be a better electron trap facilitating the charge transfer process and changing its energetics.

The effect of light on the pentane cracking in the presence of oxygen suggests that this process also might be initiated by the charge transfer in surface donor–acceptor complexes with the formation of very unstable radical cations. The induction effect observed suggests successive isomerization and cracking reactions:

$$\text{n-pentane} \rightarrow \text{i-pentane} \rightarrow \text{i-butane} + \sum \text{i-hexanes.}$$

In the case of near UV irradiation (365 nm) the induction period was less evident. Together with the observed slight increase of the isomerization activity, this suggests that pentane can be directly involved in the transformations via the radical cation mechanism under UV irradiation.

The formation of isobutane and isomeric hexanes in close amounts proves that the light-induced cracking process proceeds via C_{10} intermediates and should be better referred to as disproportionation. The formation of analogous intermediates has been suggested for the n-butane isomerization on sulfated zirconia promoted with iron and manganese (43, 44). In our case, this mechanism seems to play a secondary role in the pentane isomerization, which is likely to follow a traditional ionic mechanism. The lack of the illumination effect on the pentane isomerization makes the involvement of radical cation intermediates in this reaction unlikely, but not completely excluded.

To prove that the isomerization and disproportionation reactions observed are true catalytic reactions and not just surface stoichiometric ones, it is necessary to evaluate turnover numbers. As we did not observe pentane radical cations or immediate radical products of their chemical transformations, the concentration of strong surface acceptor sites involved in light-induced disproportionation has to be evaluated from the maximum concentration of benzene dimer radical cations in the absence of oxygen. This concentration on the active sample is 2.9×10^{16} spins/g, and such sites are not present on the inactive sample. Using this number, the turnover number for the formation of isobutane under illumination with green light can be estimated to be about 17000. This value is high enough to consider this reaction photocatalytic even despite the roughness in the evaluation of the number of active sites.

As discussed above, strong surface acceptor sites are hardly directly responsible for the isomerization activity. For evaluation of the number of active sites, we can use, for example, literature data on selective poisoning of butane isomerization over sulfated zirconia with ammonia (16). In that study ammonia adsorption in the concentration of about 50 μmol/g was sufficient to lower the isomerization activity of a sulfated zirconia catalyst prepared by a similar procedure by more than an order of magnitude. If we use this value as an estimation of the number of active sites, we shall obtain the turnover number of 1000. This is high enough to consider the reaction catalytic. It is also important to mention that in both cases there was no trend to a decrease of the reaction rate. Thus, the turnover number reached could be significantly increased.

The observed existence of a qualitative correlation between the presence of the strongest acceptor sites and the isomerization activity suggests that the acceptor sites may still be important for the activity generation. A more detailed investigation of this correlation is currently under way. We have not managed so far to detect any alkane radical cations, which are very unstable, in our system. Attempts to stabilize them will be continued.

Further studies on Fe and Mn-promoted sulfated zirconia also seem to be very important. Extensive studies of this system proved that a unique enhancement of the catalytic activity by the promotion is not related to acidity (42, 44). A potential role of strong acceptor sites and radical cation intermediates has to be elucidated.

ACKNOWLEDGMENTS

The authors are grateful to Dr. K. J. Klabunde for permission to use BET, TGA, and XRD instruments at Kansas State University. Dr. G. A. Zenkovets is thanked for synthesis of the catalysts. This work was supported in part by the Russian Foundation for Basic Research under Grants 94-03-08690 and 97-03-32566.

REFERENCES

1. Ebitani, K., Konishi, J., and Hattori, H., *J. Catal.* **130**, 257 (1991).
2. Broiwer, D. H., *J. Catal.* **1**, 372 (1962).
3. Vishnetskaya, N. V., and Romanovskii, B. V., *Zh. Fiz. Khim.* **67**, 933 (1993).
4. Romanovskii, B. V., and Vishnetskaya, N. V., *Catal. Lett.* **29**, 325 (1994).
5. Farcasiu, D., Ghenciu, A., and Li, J. Q., *J. Catal.* **158**, 116 (1996).
6. Ghenciu, A., and Farcasiu, D., *Catal. Lett.* **44**, 29 (1997).
7. Hino, M., Kobayashi, S., and Arata, K., *J. Am. Chem. Soc.* **101**, 6439 (1979).
8. Arata, K., *Adv. Catal.* **37**, 165 (1990).
9. Yamaguchi, T., *Appl. Catal.* **61**, 1 (1990).
10. Nascimento, P., Akratopoulou, C., Oszgyan, M., Coudurier, G., Travers, C., Joly, J.-F., and Vedrine, J. C., *in* "Proceedings of the 10th International Congress on Catalysis, Budapest, 1992" (L. Guzsi *et al.*, Eds.), Vol. B, p. 1185. Akademiai Kiado, Budapest, 1993.
11. Chen, F. R., Coudurier, G., Joly, J.-F., and Vedrine, J. C., *J. Catal.* **143**, 616 (1993).
12. Morterra, C., Cerrato, G., Pinna, F., and Signoretto, M., *J. Catal.* **157**, 109 (1995).
13. Ward, D. A., and Ko, E. I., *J. Catal.* **159**, 321 (1995).
14. Mastikhin, V. M., Nosov, A. V., Filimonova, S. V., Terskikh, V. V., Kotsarenko, N. S., Shmachkova, V. P., and Kim, V. I., *J. Mol. Catal. A: Chem.* **101**, 81 (1995).
15. Fogash, K. B., Yaluris, G., Gonzalez, M. R., Ouraipryvan, P., Ward, D. A., Ko, E. I., and Dumesic, J. A., *Catal Lett.* **32**, 241 (1995).
16. Yaluris, G., Larson, R. B., Kobe, J. M., Gonzalez, M. R., Fogash, K. B., and Dumesic, J. A., *J. Catal.* **158**, 336 (1996).
17. Jin, T., Yamaguchi, T., and Tanabe, K., *J. Phys. Chem.* **90**, 4794 (1986).
18. Vedrine, J. C., Auroux, A., Bolis, V., Dejaifve, P., Naccache, C., Wierzchowski, P., Derouane, E. G., Nagy, J. B., Gilson, J.-P., van Hooff, J. H. C., van den Berg, J. P., and Wolthuizen, J., *J. Catal.* **59**, 248 (1979).
19. Bolshov, V. A., and Volodin, A. M., *React. Kinet. Catal. Lett.* **43**, 87 (1991).
20. Volodin, A. M., Bolshov, V. A., and Konovalova, T. A., *Molec. Eng.* **4**, 201 (1994).
21. Timoshok, A. V., Bedilo, A. F., and Volodin, A. M., *React. Kinet. Catal. Lett.* **59**, 165 (1996).
22. Bolshov, V. A., and Volodin, A. M., *React. Kinet. Catal. Lett.* **46**, 337 (1992).
23. Bolshov, V. A., Volodin, A. M., Zhidomirov, G. M., Shubin, A. A., and Bedilo, A. F., *J. Phys. Chem.* **98**, 7551 (1994).
24. Bedilo, A. F., Volodin, A. M., Zenkovets, G. A., and Timoshok, G. V., *React. Kinet. Catal. Lett.* **55**, 183 (1995).
25. Gordon, A. J., and Ford, R. A., "The Chemist's Companion," Wiley, New York/London/Sydney/Toronto, 1972.
26. Ward, D. A., and Ko, E. I., *Chem. Mater.* **5**, 956 (1993).
27. Bedilo, A. F., and Klabunde, K. J., *Nanostruc. Mater.* **8**, 119 (1997).
28. Srinivasan, R., Harris, M. B., Simson, S. F., De Angelis, K. J., and Davis, B. H., *J. Mater. Res.* **3**, 787 (1988).
29. Srinivasan, R., Keogh, R. A., Milburn, D. R., and Davis, B. H., *J. Catal.* **153**, 123 (1995).
30. Bedilo, A. F., and Klabunde, K. J., submitted for publication.
31. Loktev, M. V., and Slinkin, A. A., *Uspekhi Khimii* **45**, 1596 (1976).
32. Afanasiev, P., Geantet, C., Breysse, M., Coudurier, G., and Vedrine, J. C., *J. Chem. Soc. Faraday Trans.* **90**, 193 (1994).
33. Kurita, Y., Sonoda, T., and Sato, M., *J. Catal.* **19**, 82 (1970).
34. Bolshov, V. A., Toktarev, A. M., and Volodin, A. M., *Mendeleev Comm.* 212 (1994).
35. Hulme, R., and Symons, M. C. R., *J. Chem. Soc.* **2**, 1120 (1965).
36. Che, M., and Tench, A. J., *Adv. Catal.* **32**, 1 (1983).
37. Komatsu, T., and Lund, A., *J. Phys. Chem.* **76**, 1727 (1972).
38. Blatter, F., and Frei, H., *J. Am. Chem. Soc.* **116**, 1812 (1994).
39. Blatter, F., Sun, H., and Frei, H., *Chem. Eur. J.* **2**, 385 (1996).
40. Bard, A. J., Ledwith, A., and Shine, H. J., *Adv. Phys. Org. Chem.* **13**, 155 (1976).
41. Bensitel, M., Saur, O., and Lavalley, J. C., *Mater. Chem Phys.* **17**, 29 (1987).
42. Tabora, J. E., and Davis, R. J., *J. Chem. Soc. Faraday Trans.* **91**, 1825 (1995).
43. Zarkalis, A. S., Hsu, C.-Y., and Gates B. C., *Catal. Lett.* **29**, 235 (1994).
44. Adeeva, V., de Haan, J. W., Janchen, J., Lei, G. D., Schunemann, V., van de Ven, L. J. M., Sachler, W. M. H., and van Santen, R. A., *J. Catal.* **151**, 364 (1995).